# *AKT3* Gene Transfer Promotes Anabolic Reprogramming and Photoreceptor Neuroprotection in a Pre-clinical Model of Retinitis Pigmentosa

Devin S. McDougald,[1] Tyler E. Papp,[1] Alexandra U. Zezulin,[1] Shangzhen Zhou,[1] and Jean Bennett[1]

[1]Center for Advanced Retinal and Ocular Therapeutics, F.M. Kirby Center for Molecular Ophthalmology, Perelman School of Medicine, University of Pennsylvania, Philadelphia, PA 19104, USA

**Mutations within over 250 known genes are associated with inherited retinal degeneration. Clinical success following gene-replacement therapy for congenital blindness due to *RPE65* mutations establishes a platform for the development of downstream treatments targeting other forms of inherited ocular disease. Unfortunately, several challenges relevant to complex disease pathology and limitations of current gene-transfer technologies impede the development of related strategies for each specific form of inherited retinal degeneration. Here, we describe a gene-augmentation strategy that delays retinal degeneration by stimulating features of anabolic metabolism necessary for survival and structural maintenance of photoreceptors. We targeted two critical points of regulation in the canonical insulin/AKT/mammalian target of rapamycin (mTOR) pathway with AAV-mediated gene augmentation in a mouse model of retinitis pigmentosa. AAV vectors expressing the serine/threonine kinase, *AKT3*, promote dramatic preservation of photoreceptor numbers, structure, and partial visual function. This protective effect was associated with successful reprogramming of photoreceptor metabolism toward pathways associated with cell growth and survival. Collectively, these findings underscore the importance of AKT activity and downstream pathways associated with anabolic metabolism in photoreceptor survival and maintenance.**

## INTRODUCTION

Retinitis pigmentosa (RP) is a collection of inherited retinal dystrophies affecting an estimated 1:3,000–7,000 individuals globally.[1] Clinical onset is characterized by impairments in scotopic (night) vision coinciding with the malfunction and then death of rod photoreceptors. As this process expands, it destroys peripheral vision and culminates in total blindness due to degeneration of cone photoreceptors in the central retina.[2] In many cases, this phenotype results from a null mutation within genes essential for rod photo-transduction, structure, or homeostasis, thus providing a direct explanation for the loss of this photoreceptor subtype. However, these mutations typically do not account for the gradual deterioration of cones in later-stage disease. These secondary degenerative events likely occur through a combination of environmental insults introduced following rod death, including increased oxidative damage, loss of rod-medi-ated trophic support, and microglial activation.[2–5] A more recently described mechanism of cone loss involves metabolic imbalance due to insufficient or impaired nutrient uptake and accompanying changes in cellular metabolism.[2,6] Following rod death, cones display features of prolonged nutrient starvation, such as increased markers of autophagy and transcriptional downregulation in critical biosynthetic pathways, particularly those controlled by mammalian target of rapamycin (mTOR) signaling activity. Systemic administration of insulin alleviates cone atrophy in a transient manner, suggesting stimulation of cell growth pathways may contribute to cone protection.[6] Furthermore, transgenic ablation of upstream suppressors in the mTOR signaling cascade mediates enhanced cone and rod photoreceptor survival in pre-clinical models of RP.[7,8]

In the present study, we questioned whether stimulation of the mTOR signaling pathway using a gene-augmentation strategy could delay photoreceptor death and preserve visual function in a pre-clinical model of inherited vision loss. We focused on two critical points of regulation in the mTOR pathway. AKT is a serine/threonine kinase responsible for cell survival and biosynthetic responses via phosphorylation of diverse protein targets including p53, FoxO/FH transcription factors, and CREB.[9] AKT stimulates mTOR activity via direct inhibitory phosphorylation of tuberin (TSC2), which functions as a potent suppressor of mTOR.[10] Prior investigations highlight the neuroprotective potential of reprogramming cell metabolism in neurodegenerative disease models by direct stimulation of AKT activity via pharmacological induction or gene augmentation.[11–13] Further downstream in the signaling cascade, mTORC1 is directly activated by the Ras homolog enriched in brain (Rheb). This is a small GTPase that cycles between active (GTP bound) and inactive (GDP bound) states based on cellular nutrient and energy availability.[14] TSC2 functions as a GTPase-activating protein (GAP) and regulates Rheb activity via direct interaction.[15] Inhibition of tuberous sclerosis

**Correspondence:** Jean Bennett, Center for Advanced Retinal and Ocular Therapeutics, F.M. Kirby Center for Molecular Ophthalmology, Perelman School of Medicine, University of Pennsylvania, 309C Stellar-Chance Laboratories, 422 Curie Blvd., Philadelphia, PA 19104, USA.
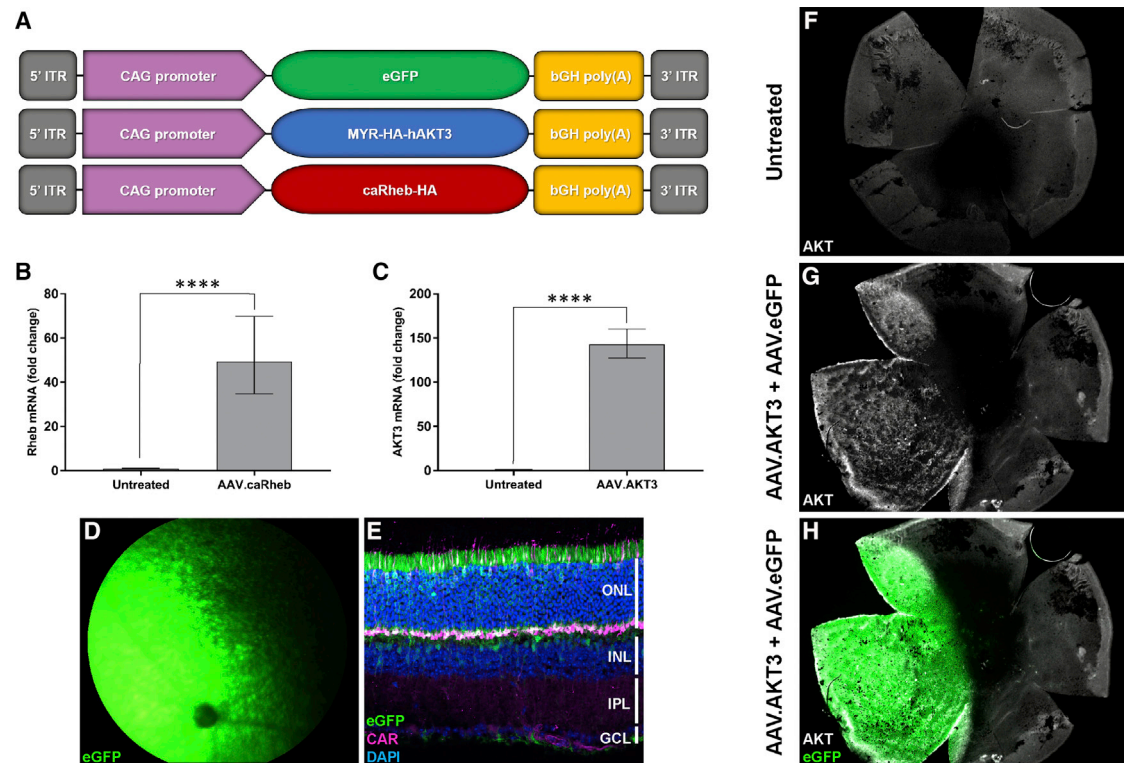**E-mail:** jebennet@pennmedicine.upenn.edu

**Figure 1. Design and Characterization of AAV7m8 Vectors**

(A) Outline of vector expression cassettes. Quantification of (B) Rheb mRNA and (C) AKT3 mRNA expression following transduction of 84-31 cells compared to untreated controls. Data represented as mean ± SD (n = 3). ****p < 0.0001. (D) Representative fundus image of mouse retina following subretinal delivery of AAV7m8.eGFP ($2 \times 10^9$ vg). (E) Retinal tropism of AAV7m8 following subretinal injection. PN45 $Pde6b^{rd10}$ retinal flatmounts stained with antibodies directed against AKT that were untreated (F) and co-injected with AAV.AKT3 ($1 \times 10^9$ vg) (G) and AAV.eGFP ($1 \times 10^9$ vg) (H).

complex (TSC) members allows Rheb to function predominantly in its active state, thereby providing potent and specific stimulation of mTORC1.[14] Previous studies observed therapeutic effects following overexpression of a constitutively active Rheb mutant (caRheb) in models of CNS injury and neurodegeneration.[16–20]

We investigated the effects of *AKT3* or *caRheb* overexpression in the $Pde6b^{rd10}$ (*rd10*) mouse model of RP. Disease in this model results from a point mutation in the gene encoding the β-subunit of rod phosphodiesterase (PDE), which renders the PDE complex non-functional and generates a blockade in the rod photo-transduction cascade.[21] Furthermore, PDE plays a critical role in the recycling of cyclic guanosine monophosphate (cGMP) to GMP, thereby facilitating the closure of voltage-gated ion channels. Loss of PDE complex activity promotes the constitutive influx of $Na^+$ and $Ca^{2+}$ ions and activation of cell death cascades.[22] $Pde6b^{rd10}$ mice display progressive thinning of the photoreceptor outer nuclear layer (ONL) beginning near postnatal day 18 (PN18). By PN30, there is significant photoreceptor loss in central and peripheral regions of the retina and typically one layer of aberrant cone cell bodies remains in the central retina at PN45.[23] In the present study, we assessed the neuroprotective potential of *AKT3* or *Rheb* delivery on visual function, structural

morphology, and preservation of photoreceptors. We further investigated potential mechanisms of any neuroprotective effect by examining the expression of markers indicative of mTOR activation. In addition, we examined the long-term safety with respect to the potential that *AKT3* or *Rheb* overexpression might lead to the oncogenic proliferation of retinal neurons.

## RESULTS

### Design and Characterization of AAV7m8 Vectors

Gene-transfer vectors derived from adeno-associated virus (AAV) have emerged as the optimal gene-delivery platform for targeting neuronal tissue. AAV7m8 is a variant of AAV2 generated through *in vivo* selection and displays enhanced retinal and cellular transduction properties.[24,25] We generated AAV7m8 vectors encoding a hyperactive version of human AKT3 (AAV.AKT3), a constitutively active Rheb mutant (AAV.caRheb), and an enhanced green fluorescent protein reporter (AAV.eGFP) as control (Figure 1A). The AKT3 transgene contains an N-terminal myristoylation (MYR) sequence, thereby enhancing membrane targeting and localization.[26] The caRheb transgene contains the canonical S16H mutation, which confers resistance to TSC-mediated GAP activity.[27] 84-31 cells transduced with the AAV.caRheb or AAV.AKT3 vectors display robust
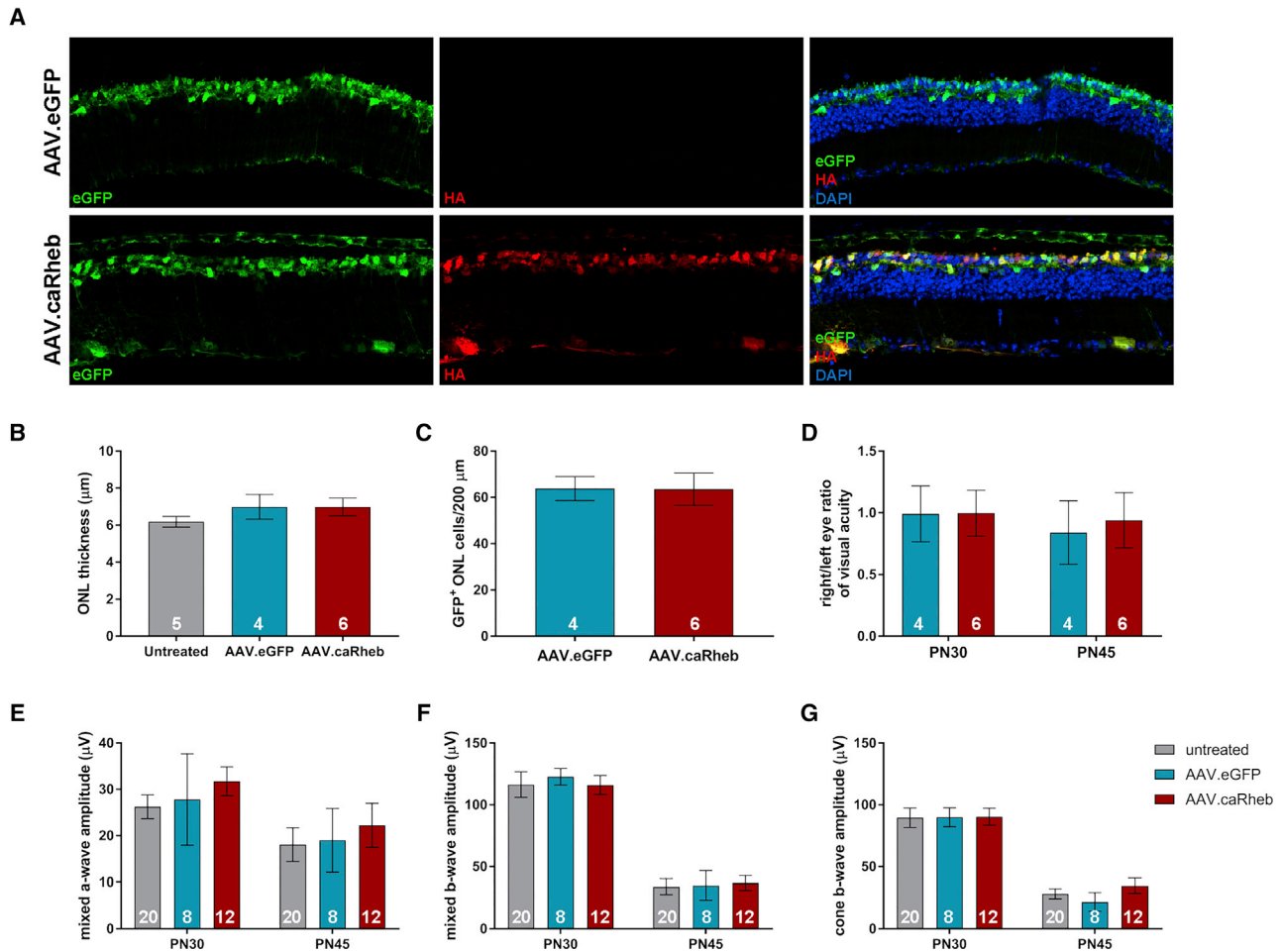
**Figure 2.** *caRheb* Augmentation Fails to Attenuate Photoreceptor Degeneration

(A) *Pde6b*^rd10 retinal cross-sections at PN45 after subretinal injection with AAV.eGFP or AAV.caRheb (plus AAV.eGFP) at PN13–14. (B) Quantification of total ONL thickness of *Pde6b*^rd10 retina treated with AAV.eGFP, AAV.caRheb/AAV.eGFP, or untreated. (C) Quantification of GFP⁺ ONL cells per 200 μm from eyes treated with AAV.eGFP alone ($2 \times 10^9$ vg) or co-injection with AAV.eGFP ($1 \times 10^9$ vg) and AAV.caRheb ($1 \times 10^9$ vg). (D) Opto-kinetic reflex (OKR) right/left ratio to assess visual acuity. Electroretinogram (ERG) measurements of the (E) mixed rod-cone A-wave amplitude, (F) mixed rod-cone B-wave amplitude, and (G) cone B-wave amplitude for the different treatments. Data represent mean ± SEM. Index indicated as the numerical values within the data bars.

expression of target gene mRNA compared to untreated controls (Figures 1B and 1C). Subretinal delivery of AAV7m8 results in robust labeling of photoreceptors, retinal pigment epithelium (RPE), and Müller cells in the mouse retina (Figures 1D and 1E). Co-injection of an experimental vector with a reporter vector results in localization of transgene expression specifically to the area of subretinal delivery (Figures 1G and 1H) allowing adequate identification of the treated retinal region.

### *caRheb* Gene Transfer Fails to Attenuate Retinal Degeneration in the *Pde6b*^rd10 Mouse

We investigated the effect of *caRheb* gene augmentation in the *Pde6b*^rd10 retina. Animals received unilateral subretinal injection of AAVs carrying the experimental transgene along with AAV containing eGFP (so that the injected portion of the retina could be identi-

fied) at PN13–14, a time point prior to the onset of rod death. Controls included injection of the eGFP containing AAV alone or no injection of AAV. Following injection, visual function was measured with electroretinogram (ERG) and optokinetic response (OKR). Retinal histology was examined at PN45 to determine the effects of AAV.caRheb on photoreceptor survival (Figures 2A–2C). Quantification of total ONL thickness per retina showed no significant difference in number of remaining photoreceptor cell bodies in experimental versus control treatments (untreated or injected with AAV.eGFP alone) (Figure 2B). In addition to total ONL thickness, we measured the number of GFP⁺ ONL cells per 200-μm sections of regions in retina transduced with AAV.eGFP alone or co-transduced with AAV.caRheb. Once again, we did not observe statistically significant changes in ONL cell numbers between these groups (Figure 2C). Furthermore, AAV.caRheb did not preserve
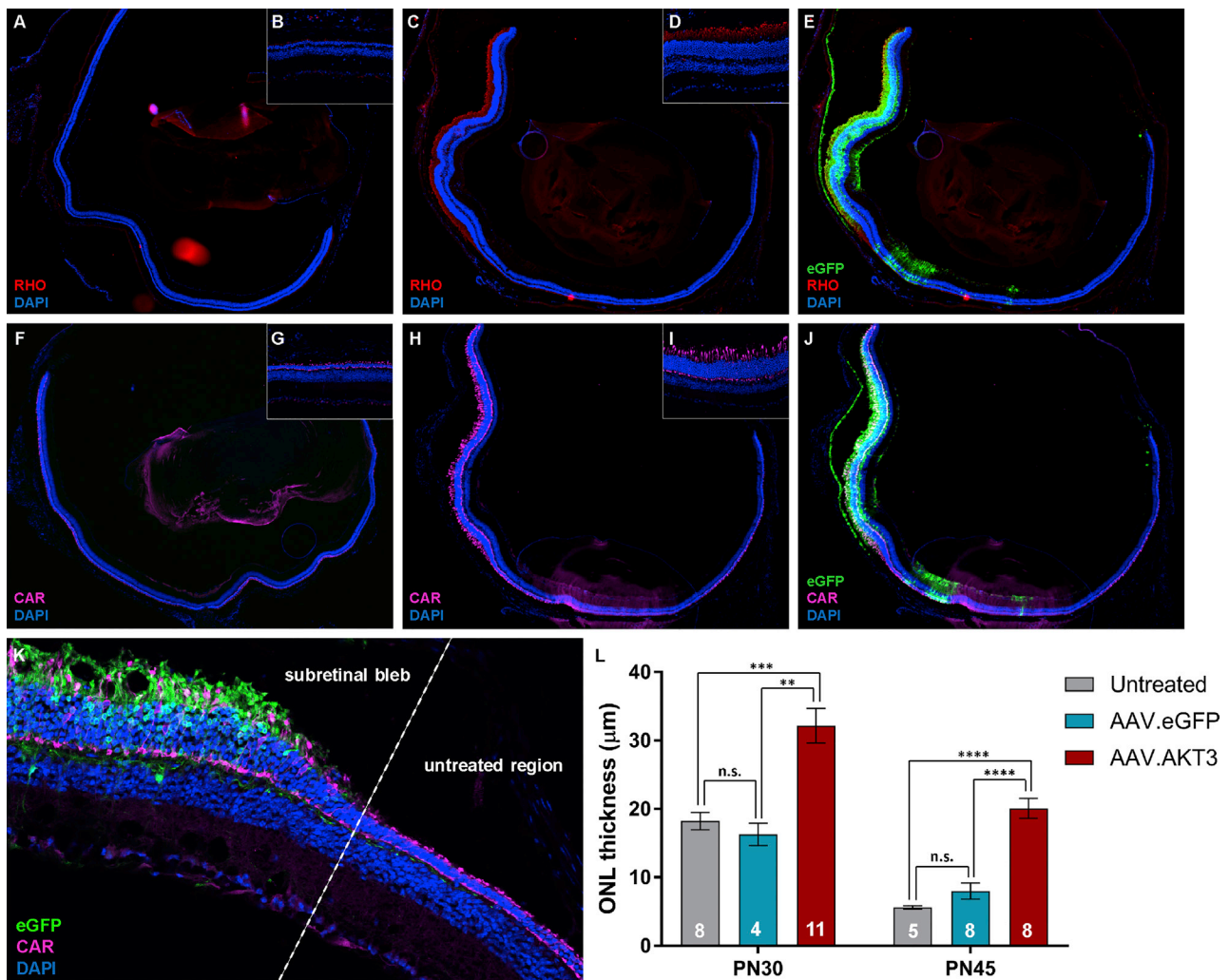
**Figure 3.** ***AKT3* Gene Transfer Promotes Photoreceptor Survival and Structural Preservation**

Whole retinal cross section from an untreated *Rd10* mouse (A) and 20× magnification of a peripheral region of the untreated retina (B) stained with antibodies directed against rhodopsin (RHO; red). Whole retinal cross section from an *Rd10* mouse treated with AAV vectors (C) and 20× magnification of a transduced region of the retina (D) stained with antibodies against RHO. (E) Co-localization with eGFP (green). Representative whole retinal cross section from an untreated *Rd10* mouse (F) and 20× magnification of a peripheral region of the untreated retina (G) stained with antibodies directed against cone arrestin (CAR; pink). Whole retinal cross section from an *Rd10* mouse treated with AAV vectors (H) and 20× magnification of a transduced region of the retina (I) stained with antibodies against CAR. (J) Co-localization with eGFP (green). (K) Representative image of the transitional region between untreated portion of the retina and subretinal bleb at PN45. (L) Quantification of ONL thickness between treatment groups at PN30 and PN45. Data represented as mean ± SEM. **p < 0.01; ***p < 0.001; ****p < 0.0001; n.s., non-significant.

retinal or visual function compared to controls as measured with ERG (Figures 2D–2F) and OKR (Figure 2G), respectively. Collectively, these data suggest caRheb gene transfer does not promote photoreceptor neuroprotection in the *Pde6b^{rd10}* mouse retina.

### *AKT3* Gene Augmentation Promotes Photoreceptor Survival and Structural Preservation in the *Pde6b^{rd10}* Retina

We examined the effect of *AKT3* gene augmentation on photoreceptor survival and structural integrity in the *Pde6b^{rd10}* retina. Histological analysis of retinal architecture at PN30 and PN45 after injection of AAV.AKT3 at PN13–14 revealed a potent neuroprotec-

tive effect on photoreceptors (as reflected by immunostaining and ONL measurements between treatment groups) specifically in retinal regions co-labeled with eGFP (Figure 3). There was no evidence of histologic rescue in AAV.GFP-injected eyes compared to untreated eyes at any time point. Immunostaining in order to probe the specific types of photoreceptors that were maintained revealed preservation of cone photoreceptors (as assessed by staining for cone arrestin) in retinal regions transduced with the AAV.AKT3 vector (Figures 3F–3J). Similarly, immunostaining for rhodopsin revealed preservation of rod photoreceptors in AAV.AKT3-transduced regions (but not unexposed regions of the retina or AAV.eGFP or untreated
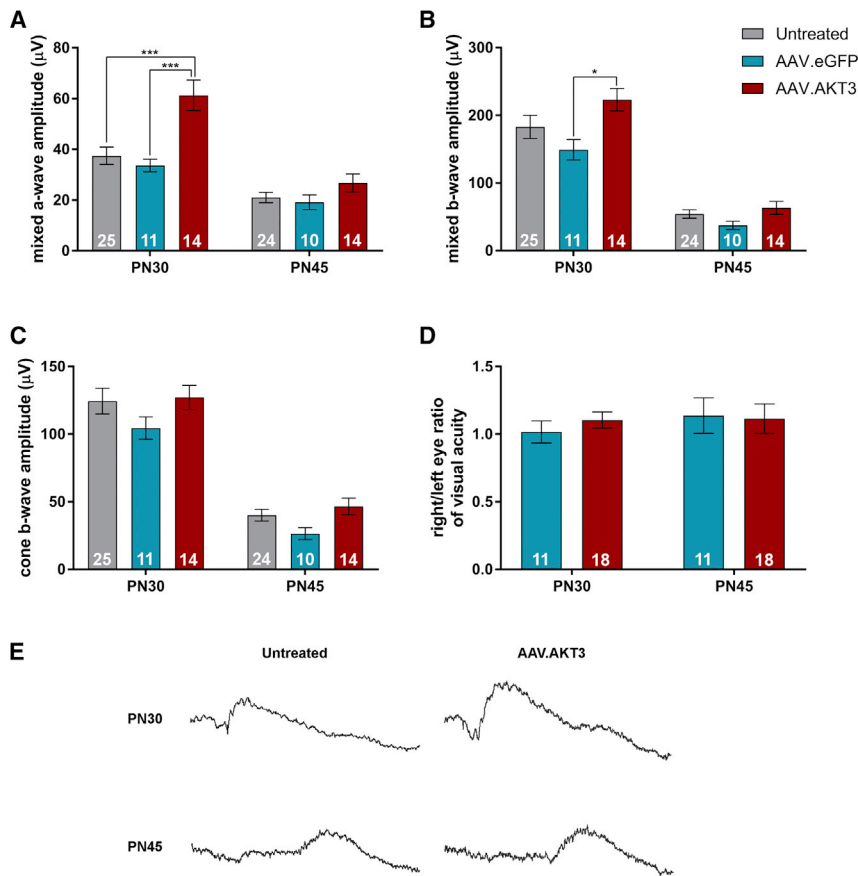
**Figure 4. Effect of *AKT3* Gene Transfer on Retinal and Visual Function in the *Pde6b^rd10* Retina**

(A) Evaluation of mixed rod-cone a-wave amplitudes between untreated, AAV.eGFP, and AAV.AKT3-treated retina. (B) Assessment of mixed rod-cone b-wave amplitudes between treatments. (C) Photopic (cone) b-wave amplitudes between treatment groups. (D) Right/left eye ratio of visual acuity examined by optokinetic response (OKR). Right eyes were treated with AAV7m8.eGFP alone (2 × 10⁹ vg) or in combination with AAV.AKT3 while left eyes were untreated. (E) Representative mixed rod-cone ERG traces at PN30 and PN45 in a *rd10* mouse treated with AAV.AKT3 in one eye and its contralateral untreated eye. Data represent mean ± SEM. *p < 0.05; ***p < 0.001. Index indicated by numerical values within bars.

control retinas). Remarkably, immunostaining for rhodopsin also revealed enhanced preservation of rod outer segments at the PN30 harvest point compared to controls, suggesting the importance of this pathway in mediating survival and maintenance of rod photoreceptor ultrastructure (Figures 3A–3E).

### Effect of *AKT3* Gene Transfer on Retinal and Visual Function in the *Pde6b^rd10* Retina

We assessed retinal and visual function at the PN30 and PN45 time points with ERG and OKR measurements, respectively. Analyses of mixed rod-cone responses from eyes treated with AAV.AKT3 revealed improved a-wave amplitudes (Figure 4A) compared to both untreated and AAV.eGFP-treated controls at PN30. In addition, stimulation of eyes treated with AAV.AKT3 also elicited increased mixed b-wave responses (Figure 4B) compared to the AAV.eGFP-treated eyes but only a trend toward increased preservation compared to untreated eyes at this time point. However, there were no significant differences in these outcome measures between treatment groups at PN45 (Figure 4B). We also measured the cone-specific b-wave response but did not observe statistically significant differences between treatment groups at any of the time points tested (Figure 4C). We examined visual acuity in response to gene transfer by measuring the OKR. Data represent the right/left eye ratio of these recordings, in which untreated left eyes served as within-animal controls while right
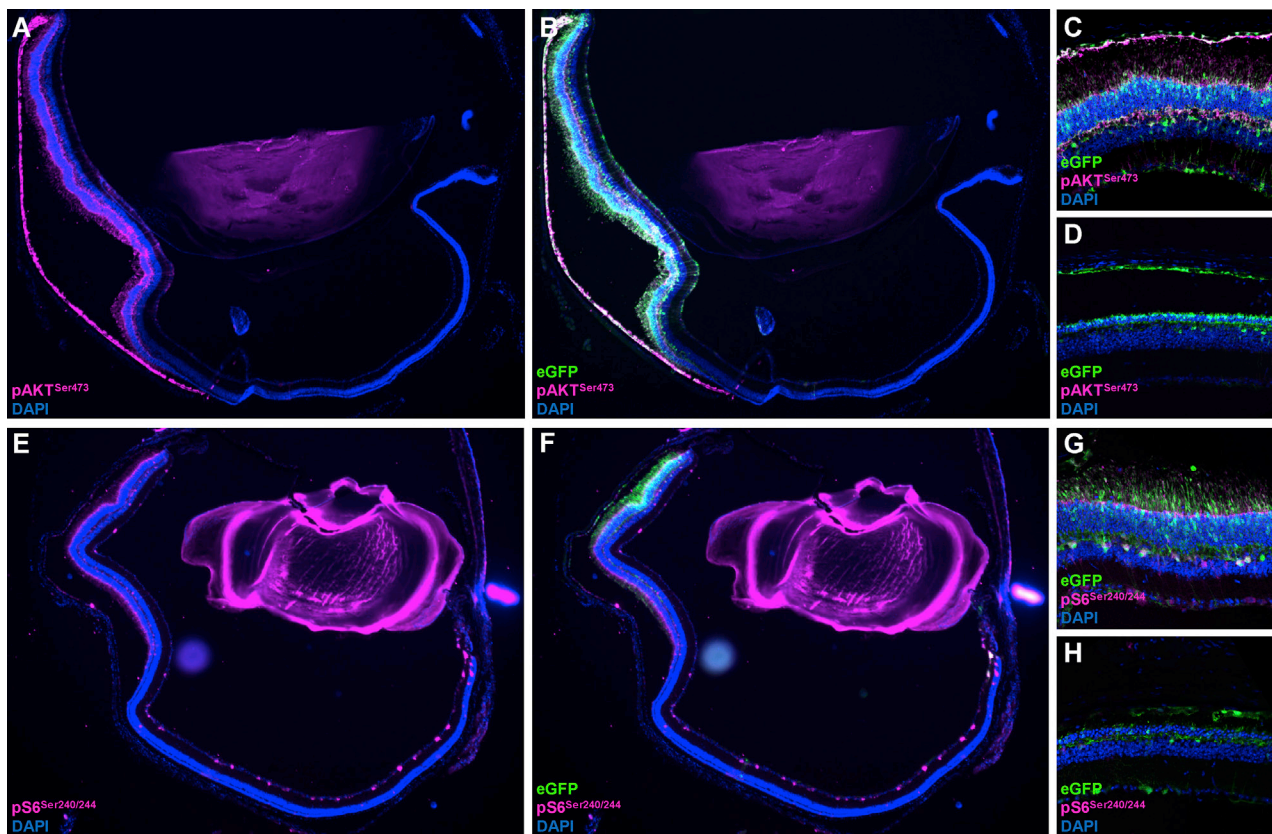
eyes were treated with AAV.eGFP alone or in combination with AAV.AKT3. Treatment with AAV.AKT3/AAV.eGFP did not preserve visual acuity relative to the AAV.eGFP control at any time point (Figure 4D). Collectively, these data indicate that AKT3 gene transfer prolongs cellular survival and some function during early- to mid-stage disease but may be insufficient for long-term maintenance.

### *AKT3* Gene Augmentation Stimulates Biosynthetic and Cell-Survival Pathways

Prior investigations underscore the contribution of mTOR in mediating photoreceptor neuroprotection in RP models.[7,8,28] We hypothesized that the AKT3-induced neuroprotective response activates pathways associated with anabolism and cell survival. In order to evaluate this possibility, we immunostained retinal sections with antibodies directed against canonical downstream markers indicative of mTOR activation (Figure 5). Regions of the retina transduced specifically with AAV.AKT3 demonstrate enhanced expression of phosphorylated ribosomal protein S6 (pS6) compared to unexposed or untreated retinas (Figures 5E–5H). This finding builds upon previous evidence suggesting the importance of mTORC1 in maintaining photoreceptor homeostasis in the degenerative retina.[7,8] Interestingly, we also observed increased expression of an mTORC2 marker (pAKT^S473) within regions specifically exposed to AAV.*AKT3*, suggesting stimulation of additional functions associated with cell survival and stress resistance (Figures 5A–5D). Retinal sections obtained from untreated and AAV.GFP control groups did not display enhanced expression of these markers, implying that AKT3-induced neuroprotection is, at least, partially driven by both the mTORC1 and the mTORC2 pathway (Figures 5D, H).

### *AKT3* Overexpression Does Not Breach Photoreceptor Quiescence but Stimulates Müller Cell Activation

Dysregulated AKT signaling is a common hallmark of many human cancers.[29] We examined the effect of *AKT3* gene transfer on retinal

**Figure 5. AKT3-Induced Neuroprotection Is Associated with mTOR Activation**

(A) Representative image of *Rd10* retina treated with AAV.AKT3/AAV.eGFP and stained with antibodies directed against the mTORC2 activation marker, phospho-AKT[Ser473] (pink). (B) Co-localization with eGFP marking the region of subretinal delivery. (C) Higher magnification of AAV.AKT3/AAV.eGFP transduced section stained with mTORC2 marker. (D) *Pde6b[rd10]* retina treated with AAV.eGFP alone and stained with the mTORC2 marker. (E) Representative image of a *Pde6b[rd10]* retina treated with AAV.AKT3/AAV.eGFP and stained for the canonical mTORC1 activation marker, phospho-S6[Ser240/244] (pink). (F) Co-localization with eGFP. (G) Higher magnification of AAV.AKT3/AAV.eGFP transduced section stained with mTORC1 marker. (H) *Pde6b[rd10]* retina treated with AAV.eGFP alone and stained with the mTORC1 marker.

quiescence by immunostaining with canonical markers of cellular proliferation. Expression of Ki67 was restricted to cells occupying the ganglion cell layer in untreated and AAV.eGFP-treated *Pde6b[rd10]* retinas. Co-staining with antibodies directed against GFAP identified this Ki67^{+} cell population as Müller glia. Under homeostatic conditions, these cells provide structural and metabolic support to other retinal cell types through mediating neurotrophic factor release, regulation of extracellular ion balance, and debris scavenging.[30,31] Importantly, cells occupying the ONL did not display positive immunoreactivity for the Ki67 marker, suggesting the AKT3-induced protective response was not a byproduct of photoreceptor quiescent escape (Figures 6H and 6I). Interestingly, Müller cells within regions of the retina specifically transduced with AAV.AKT3 demonstrate morphological changes representative of astrogliosis, such as upregulation of GFAP expression and extension of neural processes throughout different retinal layers (Figures 6G–6I). Similarly, we examined the expression of these markers in wild-type animals injected with our vector panel. Wild-type animals received subretinal injections at PN13 and were followed up for histological analysis at

PN125. We did not observe structural or cellular changes in animals harboring long-term overexpression of the reporter vector alone (Figures S2A and S2B). Conversely, animals treated with the ubiquitous AAV.AKT3 vector display extensive retinal disorganization and loss of photoreceptor structural markers (Figures S2C and S2D). Furthermore, regions specifically transduced with the AAV.AKT3 vector also display chronic activation of Müller cells compared to untreated and AAV.eGFP treated retinas (Figure 7).

**Photoreceptor-Restricted Expression of *AKT3* Mediates Neuroprotective Effects in the *Pde6b[rd10]* Retina**

We examined the effects of AKT3-mediated neuroprotection specifically within the photoreceptors by generating an AAV vector driven by the previously described *GRK1* promoter[32] (Figure 8A). Application of these vectors within the *Pde6b[rd10]* retina exerted similar effects upon retinal function as previously described vectors driven by the ubiquitous CAG promoter (Figures 8B–8D). Specifically, treatment with AAV.GRK1.AKT3 preserved mixed a-wave and b-wave amplitudes at the PN30, but not in advanced stage degeneration at PN45.
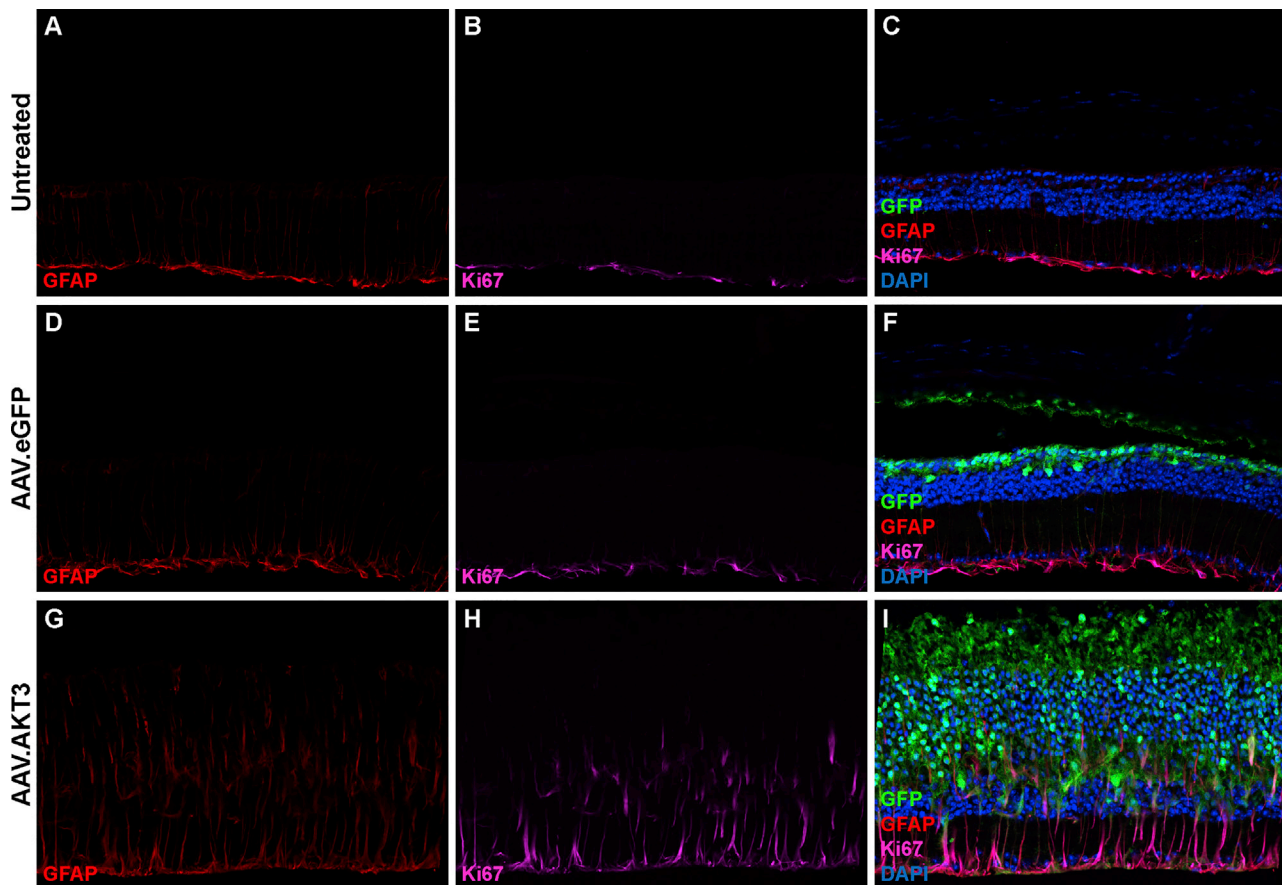
**Figure 6. *AKT3* Overexpression Does Not Breach Photoreceptor Quiescence but Activates Müller Cells**

Representative micrograph of an untreated *Pde6b^rd10* retinal cross-section stained with antibodies directed against GFAP (A), Ki67 (B), and co-localization of these markers with the addition of DAPI to identify retinal cell layers (C). Representative image of an *Rd10* mouse retina treated with AAV7m8.eGFP ($2 \times 10^9$ vg) alone and stained with antibodies directed against GFAP (D), Ki67 (E), and co-localization of these markers with the addition of DAPI to designate retinal cell layers and eGFP to identify transduced cell types (F). Representative micrograph of an *Rd10* retina co-injected with AAV7m8.eGFP ($1 \times 10^9$ vg) and AAV7m8.AKT3 ($1 \times 10^9$ vg) stained with antibodies directed against GFAP (G), Ki67 (H), and co-localization of these markers with DAPI and eGFP (I).

Similar to previous findings, these vectors did not mediate preservation of cone-specific b-wave amplitudes compared to control treatments. At the level of histology, these vectors demonstrate specific transgene expression within photoreceptors (Figure 8E). Furthermore, AAV.GRK1.AKT3 also improved photoreceptor survival compared to the untreated and AAV.eGFP treated control eyes (Figure 8F).

### AKT3 Vectors Regulated by a Photoreceptor-Specific Promoter Do Not Stimulate Reactive Gliosis in the *Pde6b^rd10* Retina

We hypothesized that restricting *AKT3* transgene expression to the photoreceptor layer with GRK1-driven vectors would abate chronic Müller cell activation observed previously with *AKT3* vectors regulated by the ubiquitous CAG promoter. Once again, we immunostained retinal sections derived from PN45 *Pde6b^rd10* mice co-injected with AAV.GRK1.AKT3 and the tracer vector with antibodies directed against GFAP and Ki67 (Figure 9). Treatment with AAV.GRK1.AKT3 did not reveal aberrant activation and migration of Müller cells in the *Pde6b^rd10* compared to untreated samples (Figures 9A–9F). Furthermore, transitional regions between untreated retinal regions and the subretinal injection site reveal similar histological findings, further suggesting that photoreceptor-restricted AKT3 gene transfer mitigates the chronic activation of Müller cells observed previously with the ubiquitous vector system (Figures 9G and 9H). These results highlight importance of cell- and tissue-specific promoters to bypass potentially detrimental off-target effects associated with neuroprotective gene-transfer strategies.

### DISCUSSION

The present study examined the therapeutic potential of reprogramming cell metabolism in an animal model of RP following stimulation of the mTOR pathway with AAV-mediated gene transfer. The exact role of mTOR signaling in the context of neurodegenerative disease remains a topic of debate. Downregulation of mTOR activity via treatment with the canonical mTOR inhibitor rapamycin can
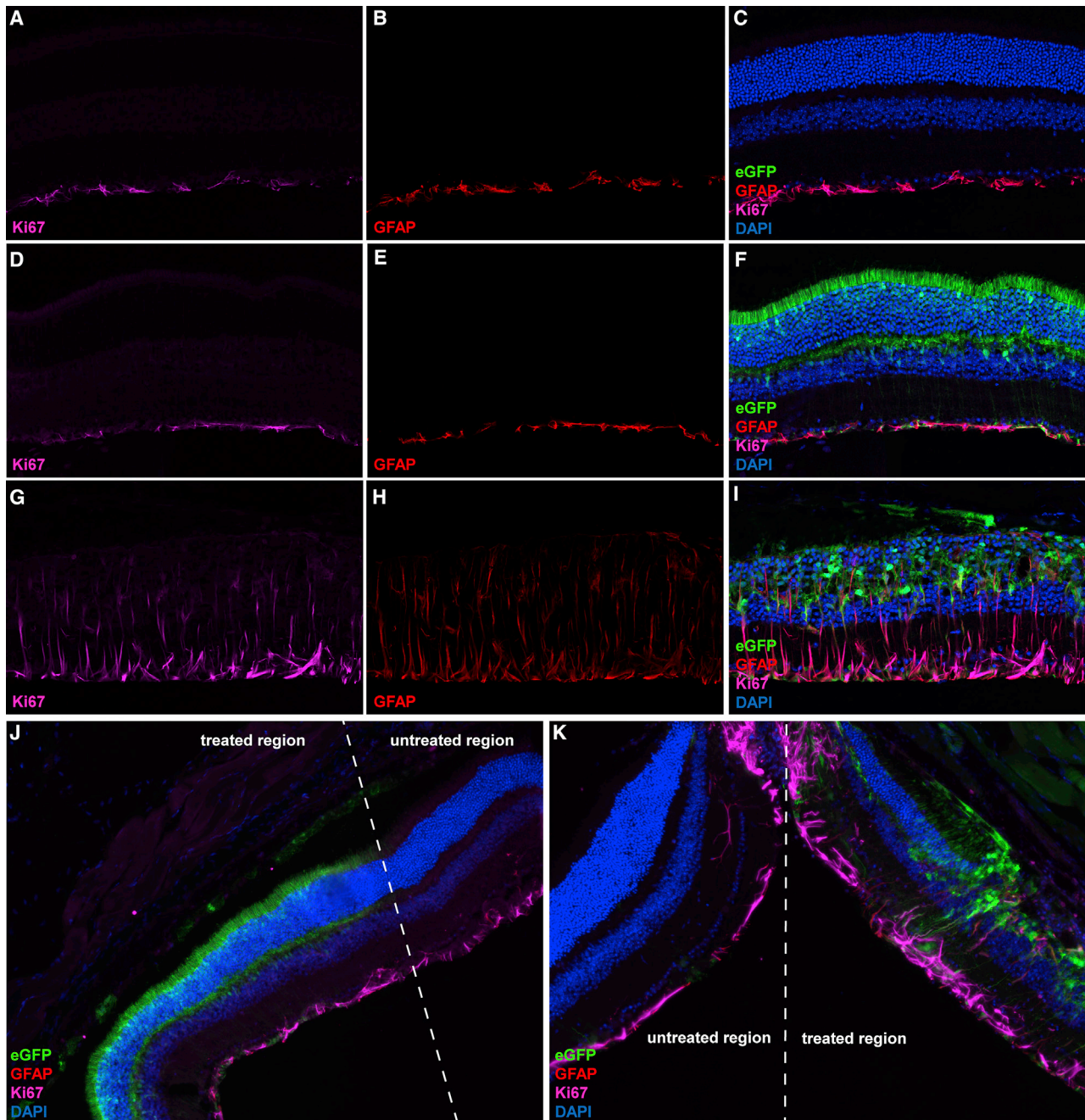
**Figure 7. Long-Term *AKT3* Gene Transfer Stimulates Chronic Müller Cell Gliosis in the Wild-Type Retina**

Representative micrographs of an untreated wild-type retinal cross sections stained with antibodies directed against Ki67 (A), GFAP (B), and co-localization with DAPI (C). Micrographs of a wild-type retina treated with AAV7m8.eGFP alone ($2 \times 10^9$ vg) and stained with antibodies against Ki67 (D), GFAP (E), and co-localization with DAPI and eGFP to designate transduced cell types (F). Micrographs acquired from wild-type retina co-injected with AAV7m8.AKT3 and AAV7m8.eGFP ($1 \times 10^9$ vg per vector) and immunostained for expression of Ki67 (G), GFAP (H), and co-localization with DAPI and eGFP to mark transduced cell types (I). (J) Transitional zone between untreated and AAV.eGFP treated retinal section. (K) Transitional zone between untreated and AAV.AKT3/AAV.eGFP treated region. All AAV injections were performed at PN13 and data was acquired from retinal tissue harvested at PN125."

attenuate pathological mechanisms in several models of neurodegeneration, including Parkinson's disease, Huntington's disease, and Alzheimer's disease.[33–36] Conversely, other investigations suggest

stimulation of the insulin/AKT/mTOR axis can mediate beneficial outcomes in related neurodegenerative disease models.[13,16,17] In the present study, targeting the mTOR pathway at two separate points
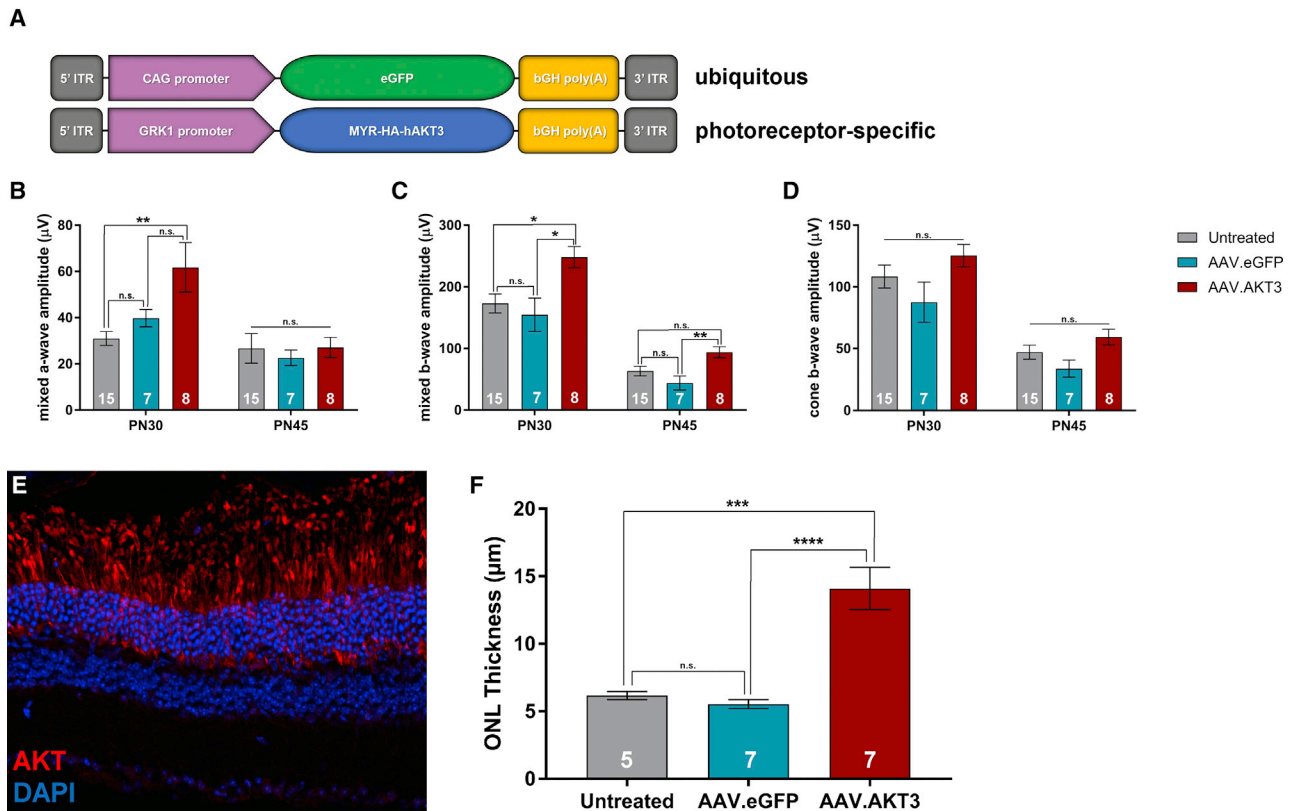
**Figure 8. Photoreceptor-Specific Expression of *AKT3* Mediates Neuroprotection in the *Pde6b^rd10* Retina**

(A) Outline of vector expression cassettes. The AKT3 transgene is regulated by the photoreceptor-specific *GRK1* promoter. Quantification of ERG responses for the (B) mixed a-wave, (C) mixed b-wave, and (D) cone b-wave between treatment groups. (E) Representative cross-section of a PN45 *Pde6b^rd10* treated with AAV7m8.GRK1.AKT3 ($1 \times 10^9$ vg). Photoreceptor-specific expression of AKT3 labeled with AKT antibodies (red). (F) Quantification of ONL thickness at PN45 between treatment groups. Data represented as mean ± SEM. *p < 0.05, **p < 0.01, ***p < 0.001, ****p < 0.0001.

of regulation led to divergent effects on photoreceptor survival, structural integrity, and retinal function.

Several studies highlight the protective potential of targeting Rheb activation to improve therapeutic outcomes in the context of neurodegenerative disease models.[16–20] Stimulating the mTOR pathway at this downstream point of regulation with *caRheb* gene transfer did not mediate a protective effect in the *Pde6b^rd10* retina. Interestingly, AAV.caRheb vectors demonstrated potent stimulation of mTORC1 activity *in vitro*, showing enhanced expression of the canonical mTORC1 activation marker, pS6. However, this activity did not translate *in vivo*, as shown by negative immunostaining for the pS6 in retinal sections overexpressing the caRheb transgene. This suggests the presence of intrinsic mechanisms to inhibit caRheb's capacity to stimulate mTORC1 within photoreceptors (Figure S1). These observations diverge from those reported in previous studies in which caRheb gene transfer stimulated mTORC1 activity within various neuronal populations and conferred stress resistance in models of Parkinson's disease, Huntington's disease, and optic nerve trauma.[16–18] Other lines of evidence suggest Rheb may play a competing role in promoting cell-death signaling programs in response to different

forms of cellular stress.[14] Ultraviolet (UV) or tumor necrosis factor alpha (TNFα)-induced cellular stress combined with *Rheb* overexpression enhanced apoptotic signaling *in vitro*, whereas *Rheb* knockdown or treatment with rapamycin provided partial protection from these cytotoxic agents.[37] In the context of retinal degeneration, light-induced damage of retinal ganglion cells (RGCs) led to upregulation in *Rheb* expression that associated with an increase in markers of apoptosis prior to degeneration.[38] Taken together, the protective or pro-apoptotic functions of Rheb are likely determined by mechanisms elicited through the specific pathology in question. Moreover, amplifying Rheb activity with gene transfer likely modulates divergent effects upon cell biology depending on the particular disease context.

AKT3 was selected based on a previous report demonstrating its increased capacity to stimulate mTORC1 activity compared to other AKT variants within retinal cell types.[12] In addition, targeted ablation of AKT3, but not AKT1 or AKT2, leads to severe neurodevelopmental defects, including reduced brain and neuron size. This suggests a unique role for this variant in neuronal homeostasis.[39] AAV-mediated *AKT3* gene transfer stimulated a potent neuroprotective effect upon photoreceptor survival and morphological preservation. This
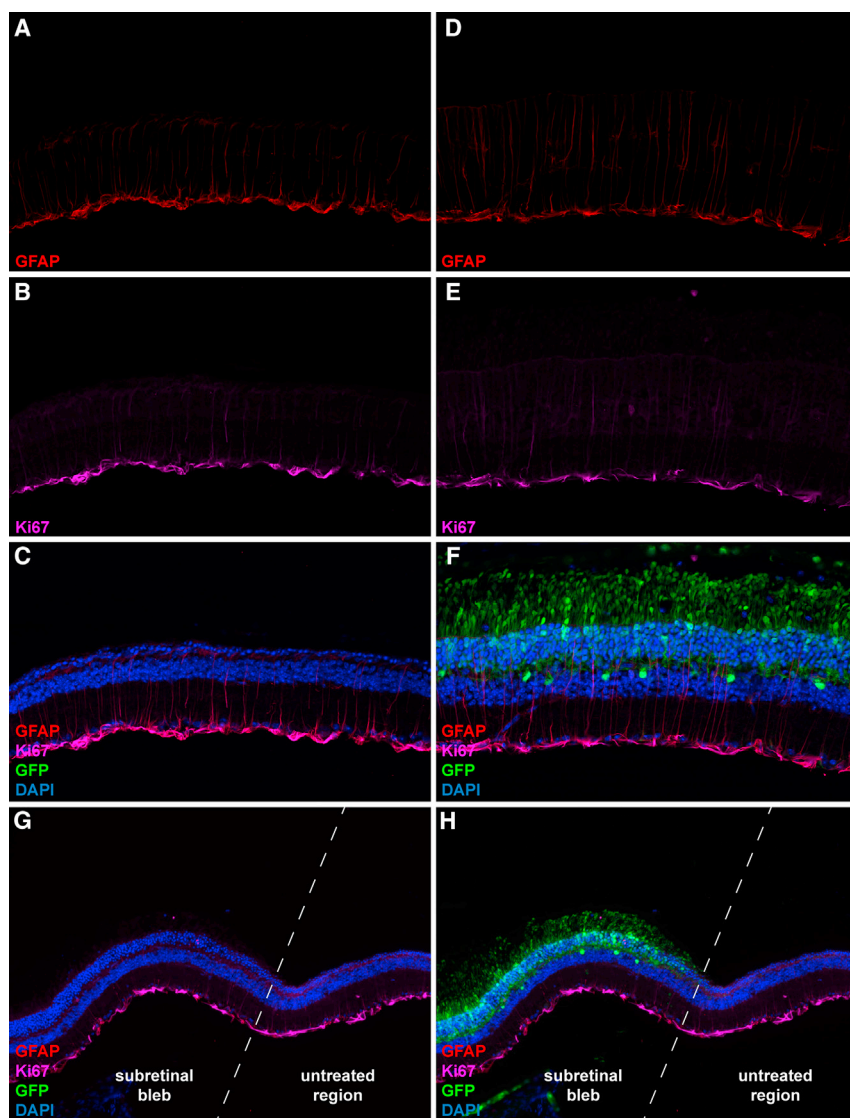
following evaluation with ERG and OKR. We observed statistically significant preservation of the mixed rod-cone a-wave and, in some cases, b-wave responses in eyes treated with CAG or *GRK1* promoter-driven AKT3 vectors at the PN30 measurement, but not during later-stage degeneration. Despite the morphological preservation of cone structure with AKT3 transgene expression, we did not observe an improvement in cone-specific light responses compared to controls at any of the time points tested. This finding deviates from prior investigations that examined strategies of cone photoreceptor neuroprotection in similar disease models.[40] These differences may be explained by variations in study design with respect not only to the transgene cassette but vector dose, injection route, kinetics of degeneration associated with the model system, and timing of vector delivery. In the present study, vectors were injected at a time point just prior to the onset of photoreceptor death, whereas previous investigations administered the experimental intervention immediately after birth and prior to retinal maturation and onset of disease mechanisms.[40] These differences in experimental design likely have important downstream implications relevant to retinal coverage, kinetics of vector recruitment, and expression in relation to onset of neurodegenerative mechanisms and ultimately therapeutic outcome measures.

Advancement of gene therapies based on strategies to reprogram cell metabolism must be met with highly stringent safety criteria prior to clinical translation. While we did not observe evidence of tumor formation, long-term overexpression of *AKT3* regulated by a ubiquitous promoter in wild-type animals led to extensive retinal disorganization and ultimately loss of photoreceptors. This phenotype corresponded with the chronic activation of Müller cells in retinal regions specifically transduced with the ubiquitous vector observed in wild-type and *Pde6b^rd10* animals. Reactive gliosis is a response typically associated with tissue injury where these cells become activated and proliferate

protective effect was associated with stimulation of mTORC1 and mTORC2 in regions of the retina specifically transduced with the AAV.AKT3 vector. While the role of mTORC1 has been extensively evaluated in RP disease models,[7,8] our findings are the first to report upregulation in mTORC2 signaling activity associated with photoreceptor neuroprotection. This data deviates from previous observations by Venkatesh et al.[7] in which mTORC2 activity was decreased following transgenic ablation of *Pten* and enhanced cone survival in the *Pde6b^rd1* mouse retina. Downstream investigations to characterize the specific contributions of mTORC1 and mTORC2 in mediating photoreceptor survival in additional animal models of inherited retinal degeneration (such as large animal models with an overall slower course of cell loss) will be crucial for clinical translation.

Despite the dramatic cellular preservation mediated by *AKT3* gene transfer, we observed differential effects upon functional preservation

to mediate various functions, including tissue remodeling, neurotrophic factor release, and scavenging of cellular debris.[30,31,41] While this response is intended to suppress further retinal damage, chronic activation may be detrimental to neighboring cells and disrupt retinal homeostasis. For example, activated Müller cells have been observed to upregulate expression and secretion of various pro-inflammatory molecules, including TNF and monocyte chemoattractant protein (MCP-1). Furthermore, they are known to secrete excess amounts of nitric oxide (NO), which generates free radicals that may be damaging to neighboring cells.[41] This finding was unsurprising, as cells require a delicate balance in these metabolic components for proper function, and excessive stimulation of these pathways will likely present detrimental effects upon cell viability. Determining and achieving this balance with gene-augmentation or -silencing strategies will be an enormous challenge in translating these approaches to the clinic. Additional regulatory elements, such as cell-specific promoters (as we showed here), stress-responsive promoters or inducible systems, will likely play critical roles in the clinical development of neuroprotective gene-transfer strategies that stimulate potent metabolic pathways. For example, Fujita et al.[42] developed an AAV vector that combined *NRF2* gene augmentation with the stress-inducible Mcp-1 promoter to provide spatial and temporal regulation of transgene expression. Other inducible systems built upon features of the *Lac* or *Tet* operon have been incorporated within AAV expression cassettes for regulation of vector expression via small-molecule induction.[43–45] Coupling such elements with *AKT* gene expression may allow "fine tuning" of downstream metabolic pathways and, importantly, provide a molecular safety switch in the event of genotoxicity or oncogenic transformation. It would also be important to evaluate dose-response effects as, here, we evaluated the effects using only one dose of the experimental reagent.

Collectively, this investigation demonstrates a broadly protective effect upon photoreceptor viability and structure following gene augmentation in a model of inherited retinal degeneration. These findings underscore the importance of AKT activity and downstream pathways associated with anabolic metabolism in photoreceptor survival and maintenance. Furthermore, the results emphasize the complex and delicate nature of reprogramming cell metabolism and important safety concerns in arresting neurodegenerative disease with "generic" gene therapy strategies.

## MATERIALS AND METHODS

### Animals
C57BL/6 and *Pde6b*[rd10] mice were obtained from the Jackson Laboratory and raised in a 12-h light/dark cycle. Animals were housed at the University of Pennsylvania in compliance with Association for Research in Vision and Ophthalmology (ARVO) guidelines on the care and use of laboratory animals as well as with institutional and federal regulations.

### AAV Vectors
A plasmid encoding the human *AKT3* cDNA sequence containing N-terminal MYR and HA tags was kindly provided by William Sellers (plasmid #9017, Addgene, Cambridge, MA). The MYR-HA-hAKT3 sequence was amplified and cloned into an AAV proviral expression plasmid using the In-Fusion HD cloning system (Clontech, Mountain View, CA, USA). The human *Rheb* cDNA clone was obtained from Origene (Rockville, MD, USA). Inverse PCR mutagenesis was employed to create the S16H mutation with the following primer sequences: 5′ [phospho]-CACGTGGGGAAATCCTCATTGAC-3′ (S16H forward) and 5′-CCGGTAGCCCAGGAT-3′. The human *Rheb* cDNA containing the S16H mutation was then cloned into an AAV proviral expression plasmid using the In-Fusion HD cloning system. For production of viral vectors, the helper plasmid expressing AAV7m8 *Cap* was kindly provided by John Flannery and David Schaffer (plasmid #64839, Addgene). AAV7m8 vectors were generated using previously described methods[46] and purified with CsCl gradient ultracentrifugation by the Center for Advanced Retinal and Ocular Therapeutics (CAROT) research vector core (University of Pennsylvania, PA, USA).

### Cell Culture and AAV Transduction
84-31 cells were kindly provided by Dr. James Wilson (University of Pennsylvania) and were cultured in DMEM-GlutaMax (Gibco, Gaithersburg, MD, USA) supplemented with 10% FBS and 1% penicillin-streptomycin (Gibco). For AAV transductions, 84-31 cells were plated at a density of $2.5 \times 10^5$ cells/well in a 6-well dish. Afterward, cells were immediately transduced with AAV7m8 vectors at $1 \times 10^6$ MOI. Cells were maintained at 37°C with 5% $CO_2$.

### RNA Isolation and Gene Expression Analysis
RNA was isolated using the Nucleospin RNA kit (Macherey-Nagel, Bethlehem, PA, USA). First-strand cDNA synthesis was performed using 500 ng of total RNA with the SuperScript III first-strand synthesis system (Thermo Fisher, Waltham, MA, USA) according to manufacturer's protocol. Real-time PCR was performed with the Applied Biosystems 7500 fast system using the power SYBR green PCR master mix (Invitrogen, Carlsbad, CA, USA). The following primer sequences were used: 5′-CCACTCCTCCACCTTTGAC-3′ (human *GAPDH* forward), 5′-ACCCTGTTGCTGTAGCCA-3′ (human *GAPDH* reverse), 5′-ACTCCTACGATCCAACCATAGA-3′ (human *Rheb* forward), 5′-TGGAGTATGTCTGAGGAAAGATAGA-3′ (human *Rheb* reverse), 5′-AGGATGGTATGGACTGCATGG-3′ (human *AKT3* forward), and 5′-GTCCACTTGCAGAGTAGGAAAA-3′ (human *AKT3* reverse). Relative gene expression was quantified with the $\Delta\Delta C_T$ method and normalized to *GAPDH*.

### Subretinal Injections
Subretinal injections were performed as previously described.[47] Each retina received 1 μL of vector preparation. Eyes that received the AAV.eGFP vector alone were dosed with $2 \times 10^9$ vector genomes. Eyes that received the combination of AAV.eGFP plus AAV.AKT3 or AAV.caRheb were dosed with $1 \times 10^9$ vector genomes per vector ($2 \times 10^9$ total vector genomes).

## ERG

Mice were anesthetized with ketamine and xylazine. Pupils were dilated with 1% tropicamide (Alcon Laboratories, Fort Worth, TX, USA). Clear plastic contact lenses with embedded platinum wires were used to record light responses, and a platinum wire loop was placed into the animal's mouth to serve as a reference electrode. ERGs were recorded with the Espion E2 system (Diagnosys, Lowell, MA, USA). Three ERG responses were recorded with the following parameters: scotopic response (dark adaption, 0.01 scot cd s $m^{-2}$ stimulus), maximum mixed rod-cone response (dark adaptation, 500 scot cd s $m^{-2}$ stimulus), maximum cone response (30 scot cd $m^{-2}$ adapting steady background light, 500 scot cd s $m^{-2}$ stimulus).

## OKR

Visual acuity was assessed by measuring the OKR using the OptoMotry software and apparatus (Cerebral Mechanics, Medicine Hat, AB, Canada) as previously described.[48] Recordings were performed by an investigator masked to the experimental treatments.

## Immunohistochemistry

Eyes were enucleated, harvested, and prepared as frozen sections as previously described.[47] Sections were incubated in blocking buffer containing PBS, 10% normal goat serum (Cell Signaling Technology, Danvers, MA, USA), and 2% Triton X-100 (Sigma-Aldrich, St. Louis, MO, USA) for 1 h at room temperature. Afterward, sections were incubated in primary antibody solution overnight in a humidified chamber containing the previously described components and combinations of the following antibodies: rabbit anti-cone arrestin (1:400; ab15282, Millipore, Burlington, MA, USA), rabbit anti-phospho-S6-Ser240/244 (1:100; 5364, Cell Signaling Technology), rabbit anti-phospho-AKT-Ser273 (1:100; 4060, Cell Signaling Technology), mouse anti-rhodopsin (1:400; ab5417, Abcam, Cambridge, UK), rabbit anti-HA (1:100; 3724, Cell Signaling Technology), rabbit anti-Ki67 (1:400; ab15580, Abcam), mouse anti-PCNA (1:400; ab29, Abcam), chicken anti-GFAP (1:400; ab4674, Abcam), and rabbit anti-AKT (1:100; 4691, Cell Signaling Technology). Following primary antibody incubation, sections were washed three times with PBS and incubated in secondary antibody solution for 2 h at room temperature in a humidified chamber containing PBS, 10% normal goat serum, 2% Triton X-100, and a combination of the following secondary antibodies: Alexa Fluor 594 goat anti-chicken (1:500; ab150176, Abcam), Alexa Fluor 594 goat anti-mouse (1:500; ab150116, Abcam), Alexa Fluor 594 goat anti-rabbit (1:500; ab150080, Abcam), Cy5-conjugated goat anti-rabbit (1:500; 072-02-15-16, Seracare, Milford, MA, USA). Sections were removed from secondary antibody incubation and washed three times with PBS. Sections stained for the presence of phosphorylated antigens were incubated and washed in solutions containing Tris-buffered saline (TBS) instead of PBS.

## ONL Measurements

Whole retinal sections were tiled using a 40× objective with the EVOS FL auto 2 cell imaging system. In each image, ONL thickness was measured at three equidistant points spaced 75–100 μm apart. These measurements were averaged between all images to represent the average ONL thickness of the section. Three retinal sections were averaged per sample. ONL numbers from specific regions of the retina transduced with vector were quantified by counting the number of GFP$^+$ ONL cells per a 200-μm area. Once again, three retinal sections were averaged per sample to acquire these measurements.

## Western Blotting

Protein samples were separated with the NuPage electrophoresis system (Thermo Fisher). Samples were heated at 70°C and loaded onto 4%–12% Bis-Tris protein gels (Thermo Fisher). Separated proteins were then transferred to a polyvinylidene fluoride (PVDF) membrane with the XCell II blot module (Thermo Fisher) at 35 V for 1.5 h. Following protein transfer, membranes were incubated in TBS containing 0.1% (v/v) Tween 20 (Bio-Rad, Hercules, CA, USA) (TBST) and 5% (w/v) BSA (Sigma-Aldrich) for 1 h at room temperature. Afterward, blots were incubated in the previously described solution containing the following primary antibodies: rabbit anti-phospho-S6-Ser240/244 (1:1,000; 5364, Cell Signaling Technology), rabbit anti-S6 (1:1,000; 2217, Cell Signaling Technology), and rabbit anti-GAPDH (1:1,000; 5174, Cell Signaling Technology). Primary antibody incubation occurred overnight at 4°C. Blots were removed from primary antibody solution and washed three times in TBST for 5 min each. Afterward, they were placed in secondary antibody solution composed of TBST, 5% BSA, and horseradish peroxidase (HRP)-conjugated anti-rabbit enhanced chemiluminescence (ECL) (1:10,000; GE Healthcare, Chicago, IL) for 1 h at room temperature. Membranes were washed three times in TBST followed by incubation with ECL2 (Thermo Fisher) according to manufacturer's instructions for 5 min. Finally, membranes were imaged using the Amersham Imager 600 (GE Healthcare) with chemiluminescence settings.

## Statistics

All data are represented as means ± SEM unless otherwise indicated. Differences between two treatment groups were compared using an unpaired Student's t test. Differences between three or more experimental groups were compared using a one-way ANOVA followed by Turkey's honest significant difference test. Calculations for statistical significance were determined using GraphPad Prism 7.0. Differences were considered statistically significant at $p < 0.05$.

## SUPPLEMENTAL INFORMATION

Supplemental Information can be found online at https://doi.org/10.1016/j.ymthe.2019.04.009.

## AUTHOR CONTRIBUTIONS

D.S.M. conceived the study, generated reagents, designed and performed experiments, collected and analyzed data, and wrote the manuscript. T.E.P. and A.U.Z. performed experiments and collected

data. S.Z. generated rAAV vectors. J.B. supervised the study. All authors edited and approved the finalized manuscript.

## REFERENCES

1. Retinal Information Network (RetNet). American Red Cross. https://sph.uth.edu/retnet.

2. Punzo, C., Xiong, W., and Cepko, C.L. (2012). Loss of daylight vision in retinal degeneration: are oxidative stress and metabolic dysregulation to blame? J. Biol. Chem. 287, 1642–1648.

3. Aït-Ali, N., Fridlich, R., Millet-Puel, G., Clérin, E., Delalande, F., Jaillard, C., Blond, F., Perrocheau, L., Reichman, S., Byrne, L.C., et al. (2015). Rod-derived cone viability factor promotes cone survival by stimulating aerobic glycolysis. Cell 161, 817–832.

4. Gupta, N., Brown, K.E., and Milam, A.H. (2003). Activated microglia in human retinitis pigmentosa, late-onset retinal degeneration, and age-related macular degeneration. Exp. Eye Res. 76, 463–471.

5. Shen, J., Yang, X., Dong, A., Petters, R.M., Peng, Y.W., Wong, F., and Campochiaro, P.A. (2005). Oxidative damage is a potential cause of cone cell death in retinitis pigmentosa. J. Cell. Physiol. 203, 457–464.

6. Punzo, C., Kornacker, K., and Cepko, C.L. (2009). Stimulation of the insulin/mTOR pathway delays cone death in a mouse model of retinitis pigmentosa. Nat. Neurosci. 12, 44–52.

7. Venkatesh, A., Ma, S., Le, Y.Z., Hall, M.N., Rüegg, M.A., and Punzo, C. (2015). Activated mTORC1 promotes long-term cone survival in retinitis pigmentosa mice. J. Clin. Invest. 125, 1446–1458.

8. Zhang, L., Justus, S., Xu, Y., Pluchenik, T., Hsu, C.W., Yang, J., Duong, J.K., Lin, C.S., Jia, Y., Bassuk, A.G., et al. (2016). Reprogramming towards anabolism impedes degeneration in a preclinical model of retinitis pigmentosa. Hum. Mol. Genet. 25, 4244–4255.

9. Manning, B.D., and Toker, A. (2017). AKT/PKB signaling: navigating the network. Cell 169, 381–405.

10. Inoki, K., Li, Y., Zhu, T., Wu, J., and Guan, K.L. (2002). TSC2 is phosphorylated and inhibited by Akt and suppresses mTOR signalling. Nat. Cell Biol. 4, 648–657.

11. Isiegas, C., Marinich-Madzarevich, J.A., Marchena, M., Ruiz, J.M., Cano, M.J., de la Villa, P., Hernández-Sánchez, C., de la Rosa, E.J., and de Pablo, F. (2016). Intravitreal injection of proinsulin-loaded microspheres delays photoreceptor cell death and vision loss in the rd10 mouse model of retinitis pigmentosa. Invest. Ophthalmol. Vis. Sci. 57, 3610–3618.

12. Miao, L., Yang, L., Huang, H., Liang, F., Ling, C., and Hu, Y. (2016). mTORC1 is necessary but mTORC2 and GSK3β are inhibitory for AKT3-induced axon regeneration in the central nervous system. eLife 5, e14908.

13. Ries, V., Henchcliffe, C., Kareva, T., Rzhetskaya, M., Bland, R., During, M.J., Kholodilov, N., and Burke, R.E. (2006). Oncoprotein Akt/PKB induces trophic effects in murine models of Parkinson's disease. Proc. Natl. Acad. Sci. USA 103, 18757–18762.

14. Potheraveedu, V.N., Schöpel, M., Stoll, R., and Heumann, R. (2017). Rheb in neuronal degeneration, regeneration, and connectivity. Biol. Chem. 398, 589–606.

15. Inoki, K., Li, Y., Xu, T., and Guan, K.L. (2003). Rheb GTPase is a direct target of TSC2 GAP activity and regulates mTOR signaling. Genes Dev. 17, 1829–1834.

16. Kim, S.R., Kareva, T., Yarygina, O., Kholodilov, N., and Burke, R.E. (2012). AAV transduction of dopamine neurons with constitutively active Rheb protects from neurodegeneration and mediates axon regrowth. Mol. Ther. 20, 275–286.

17. Lee, J.H., Tecedor, L., Chen, Y.H., Monteys, A.M., Sowada, M.J., Thompson, L.M., and Davidson, B.L. (2015). Reinstating aberrant mTORC1 activity in Huntington's disease mice improves disease phenotypes. Neuron 85, 303–315.

18. Lim, J.H., Stafford, B.K., Nguyen, P.L., Lien, B.V., Wang, C., Zukor, K., He, Z., and Huberman, A.D. (2016). Neural activity promotes long-distance, target-specific regeneration of adult retinal axons. Nat. Neurosci. 19, 1073–1084.

19. Wu, D., Klaw, M.C., Kholodilov, N., Burke, R.E., Detloff, M.R., Côté, M.P., and Tom, V.J. (2016). Expressing constitutively active rheb in adult dorsal root ganglion neurons enhances the integration of sensory axons that regenerate across a chondroitinase-treated dorsal root entry zone following dorsal root crush. Front. Mol. Neurosci. 9, 49.

20. Wu, D., Klaw, M.C., Connors, T., Kholodilov, N., Burke, R.E., Côté, M.P., and Tom, V.J. (2017). Combining constitutively active rheb expression and chondroitinase promotes functional axonal regeneration after cervical spinal cord injury. Mol. Ther. 25, 2715–2726.

21. Chang, B., Hawes, N.L., Hurd, R.E., Davisson, M.T., Nusinowitz, S., and Heckenlively, J.R. (2002). Retinal degeneration mutants in the mouse. Vision Res. 42, 517–525.

22. Wang, T., Tsang, S.H., and Chen, J. (2017). Two pathways of rod photoreceptor cell death induced by elevated cGMP. Hum. Mol. Genet. 26, 2299–2306.

23. Gargini, C., Terzibasi, E., Mazzoni, F., and Strettoi, E. (2007). Retinal organization in the retinal degeneration 10 (rd10) mutant mouse: a morphological and ERG study. J. Comp. Neurol. 500, 222–238.

24. Dalkara, D., Byrne, L.C., Klimczak, R.R., Visel, M., Yin, L., Merigan, W.H., Flannery, J.G., and Schaffer, D.V. (2013). In vivo-directed evolution of a new adeno-associated virus for therapeutic outer retinal gene delivery from the vitreous. Sci. Transl. Med. 5, 189ra76.

25. Khabou, H., Desrosiers, M., Winckler, C., Fouquet, S., Auregan, G., Bemelmans, A.P., Sahel, J.A., and Dalkara, D. (2016). Insight into the mechanisms of enhanced retinal transduction by the engineered AAV2 capsid variant -7m8. Biotechnol. Bioeng. 113, 2712–2724.

26. McIlhinney, R.A. (1998). Membrane targeting via protein N-myristoylation. Methods Mol. Biol. 88, 211–225.

27. Yan, L., Findlay, G.M., Jones, R., Procter, J., Cao, Y., and Lamb, R.F. (2006). Hyperactivation of mammalian target of rapamycin (mTOR) signaling by a gain-of-function mutant of the Rheb GTPase. J. Biol. Chem. 281, 19793–19797.

28. Tsang, S.H., Chan, L., Tsai, Y.T., Wu, W.H., Hsu, C.W., Yang, J., Tosi, J., Wert, K.J., Davis, R.J., and Mahajan, V.B. (2014). Silencing of tuberin enhances photoreceptor survival and function in a preclinical model of retinitis pigmentosa (an American ophthalmological society thesis). Trans. Am. Ophthalmol. Soc. 112, 103–115.

29. Altomare, D.A., and Testa, J.R. (2005). Perturbations of the AKT signaling pathway in human cancer. Oncogene 24, 7455–7464.

30. Goldman, D. (2014). Müller glial cell reprogramming and retina regeneration. Nat. Rev. Neurosci. 15, 431–442.

31. Reichenbach, A., and Bringmann, A. (2013). New functions of Müller cells. Glia 61, 651–678.

32. Khani, S.C., Pawlyk, B.S., Bulgakov, O.V., Kasperek, E., Young, J.E., Adamian, M., Sun, X., Smith, A.J., Ali, R.R., and Li, T. (2007). AAV-mediated expression targeting of rod and cone photoreceptors with a human rhodopsin kinase promoter. Invest. Ophthalmol. Vis. Sci. 48, 3954–3961.

33. Bové, J., Martínez-Vicente, M., and Vila, M. (2011). Fighting neurodegeneration with rapamycin: mechanistic insights. Nat. Rev. Neurosci. 12, 437–452.

34. Malagelada, C., Jin, Z.H., Jackson-Lewis, V., Przedborski, S., and Greene, L.A. (2010). Rapamycin protects against neuron death in in vitro and in vivo models of Parkinson's disease. J. Neurosci. 30, 1166–1175.

35. Ravikumar, B., Vacher, C., Berger, Z., Davies, J.E., Luo, S., Oroz, L.G., Scaravilli, F., Easton, D.F., Duden, R., O'Kane, C.J., and Rubinsztein, D.C. (2004). Inhibition of mTOR induces autophagy and reduces toxicity of polyglutamine expansions in fly and mouse models of Huntington disease. Nat. Genet. 36, 585–595.

36. Spilman, P., Podlutskaya, N., Hart, M.J., Debnath, J., Gorostiza, O., Bredesen, D., Richardson, A., Strong, R., and Galvan, V. (2010). Inhibition of mTOR by rapamycin abolishes cognitive deficits and reduces amyloid-β levels in a mouse model of Alzheimer's disease. PLoS ONE 5, e9979.

37. Karassek, S., Berghaus, C., Schwarten, M., Goemans, C.G., Ohse, N., Kock, G., Jockers, K., Neumann, S., Gottfried, S., Herrmann, C., et al. (2010). Ras homolog enriched in brain (Rheb) enhances apoptotic signaling. J. Biol. Chem. 285, 33979–33991.

38. Shu, Q., Xu, Y., Zhuang, H., Fan, J., Sun, Z., Zhang, M., and Xu, G. (2014). Ras homolog enriched in the brain is linked to retinal ganglion cell apoptosis after light injury in rats. J. Mol. Neurosci. 54, 243–251.

39. Easton, R.M., Cho, H., Roovers, K., Shineman, D.W., Mizrahi, M., Forman, M.S., Lee, V.M.Y., Szabolcs, M., de Jong, R., Oltersdorf, T., et al. (2005). Role for Akt3/protein kinase Bgamma in attainment of normal brain size. Mol. Cell. Biol. 25, 1869–1878.

40. Xiong, W., MacColl Garfinkel, A.E., Li, Y., Benowitz, L.I., and Cepko, C.L. (2015). NRF2 promotes neuronal survival in neurodegeneration and acute nerve damage. J. Clin. Invest. 125, 1433–1445.

41. Bringmann, A., Iandiev, I., Pannicke, T., Wurm, A., Hollborn, M., Wiedemann, P., Osborne, N.N., and Reichenbach, A. (2009). Cellular signaling and factors involved in Müller cell gliosis: neuroprotective and detrimental effects. Prog. Retin. Eye Res. 28, 423–451.

42. Fujita, K., Nishiguchi, K.M., Shiga, Y., and Nakazawa, T. (2017). Spatially and temporally regulated NRF2 gene therapy using Mcp-1 promoter in retinal ganglion cell injury. Mol. Ther. Methods Clin. Dev. 5, 130–141.

43. Santiago, C.P., Keuthan, C.J., Boye, S.L., Boye, S.E., Imam, A.A., and Ash, J.D. (2018). A drug-tunable gene therapy for broad-spectrum protection against retinal degeneration. Mol. Ther. 26, 2407–2417.

44. Sochor, M.A., Vasireddy, V., Drivas, T.G., Wojno, A., Doung, T., Shpylchak, I., Bennicelli, J., Chung, D., Bennett, J., and Lewis, M. (2015). An autogenously regulated expression system for gene therapeutic ocular applications. Sci. Rep. 5, 17105.

45. Zhong, G., Wang, H., Bailey, C.C., Gao, G., and Farzan, M. (2016). Rational design of aptazyme riboswitches for efficient control of gene expression in mammalian cells. eLife 5, e18858.

46. Ramachandran, P.S., Lee, V., Wei, Z., Song, J.Y., Casal, G., Cronin, T., Willett, K., Huckfeldt, R., Morgan, J.I., Aleman, T.S., et al. (2017). Evaluation of dose and safety of AAV7m8 and AAV8BP2 in the non-human primate retina. Hum. Gene Ther. 28, 154–167.

47. Dooley, S.J., McDougald, D.S., Fisher, K.J., Bennicelli, J.L., Mitchell, L.G., and Bennett, J. (2018). Spliceosome-mediated pre-mRNA trans-splicing can repair CEP290 mRNA. Mol. Ther. Nucleic Acids 12, 294–308.

48. McDougald, D.S., Dine, K.E., Zezulin, A.U., Bennett, J., and Shindler, K.S. (2018). SIRT1 and NRF2 gene transfer mediate distinct neuroprotective effects upon retinal ganglion cell survival and function in experimental optic neuritis. Invest. Ophthalmol. Vis. Sci. 59, 1212–1220.

Supplemental Information

*AKT3* Gene Transfer Promotes Anabolic

Reprogramming and Photoreceptor Neuroprotection

in a Pre-clinical Model of Retinitis Pigmentosa

Devin S. McDougald, Tyler E. Papp, Alexandra U. Zezulin, Shangzhen Zhou, and Jean Bennett

**Figure S1. AAV.caRheb stimulates mTORC1 activity *in vitro* but not in photoreceptors. (A)** Western blot evaluating expression of pS6$^{Ser240/244}$, S6, and GAPDH (loading control) from untreated 84-31 cells or treated with AAV.eGFP or AAV.caRheb. Numerical values indicate biological replicates for each treatment condition. **(B)** Representative micrographs of retinal sections injected with AAV.eGFP alone (top panels) or with AAV.caRheb/AAV.eGFP (bottom panels) and stained with antibodies directed against pS6$^{Ser240/244}$.
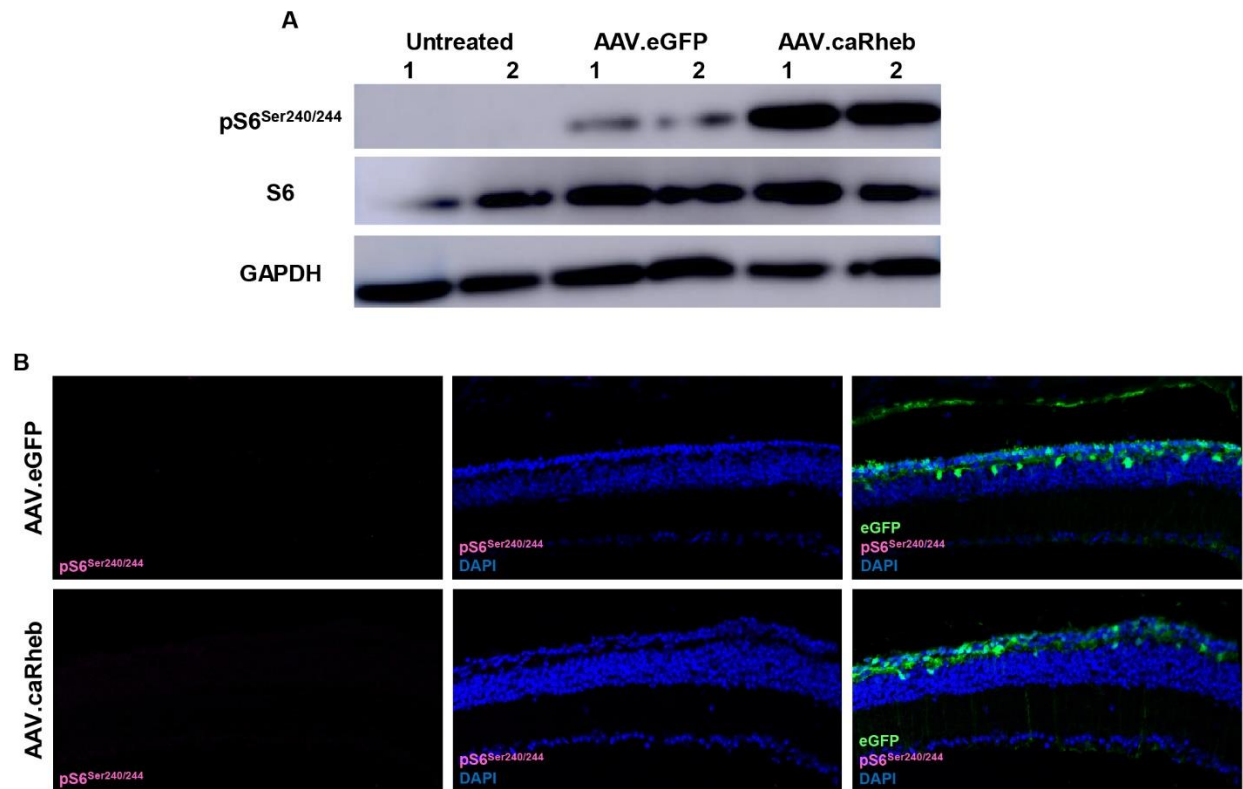
**Figure S2. Long-term *AKT3* gene transfer leads to retinal disorganization in wild-type animals.** C57Bl/6 (wild-type) mice received subretinal injection at PN13. **(A-B)** Retinal histology at PN125 reveals normal photoreceptor structure in animals treated with AAV.eGFP alone. **(C-D)** Animals treated with AAV.eGFP in combination with AAV.AKT3 display extensive disorganization of retinal layers and loss of photoreceptor numbers and structure.